Physical Experiments for Large Deformation Problems

Wan-Suk Yoo †, Jeong-Han Lee, Jeong-Hyun Sohn, Su-Jin Park

† CAELab, NRL, Pusan National University, Kumjung-Ku, Busan 609-735, South Korea, wsyoo@pusan.ac.kr

Many papers have studied computer simulations of elastic bodies undergoing large deflections and large deformations. But there have not been many attempts to check the validity of the numerical formulations because the simulation results could not be matched without correct input data such as material properties and damping effects. In this paper, these values are obtained from real experiment with a high-speed camera and a data acquisition system. The simulation results with the absolute nodal coordinate formulation (ANCF) are compared with the results of real experiments. Two examples, a thin cantilever beam and a thin plate, are studied to verify whether the simulation results are well matched to experimental results.

Key words: large displacements, experiments, simulation, absolute nodal coordinate formulation,

1. Introduction

The absolute nodal coordinate formulation (ANCF) was known a nice technique for modeling and simulation of large deformation and large displacement problems [1]. In this formulation, displacements of each finite element are represented relative to the global frame of reference. And the equations of motion with this formulation generate a constant mass matrix and a constant vector of generalized gravity forces as well as zero centrifugal and Coriolis forces [2]. Thus, the only nonlinear term in the equations of motion is the vector of elastic forces.

Although this formulation is widely used for simulations of large deformation problems with nice animations, no paper was written concerning the validity of these simulations by comparing with real experiments. Without correct input data, such as air damping in the motion, the simulation could not be well matched to the experimental results. Thus, in this paper, Young's modulus E and the damping ratio of the material used in the simulation are obtained from the real experiments. Thus, the precise validation of the ANCF could be checked. For the author's knowledge, this is the first paper to compare the ANCF formulation to real experiments. Two experiments, a 2D beam deflection and a thin plate oscillation, are carried out and compared to show the validity of the simulations.

For the modeling of a 2D beam, many models of elastic forces have been proposed which use a matrix representation of the beam shape functions and nodal coordinates [3]. In this paper, a new geometrical treatment of the absolute nodal coordinates is suggested. Nodal displacements and nodal slopes are employed for the finite element formulation. The position of an arbitrary point in the beam centerline is then expressed as a linear combination of the nodal vectors with the shape functions used as coefficients. This approach is identical to the matrix representation proposed in paper [4], but it avoids the problem of using zero values for the shape function matrix. Strain energy, elastic forces and their Jacobian matrices are calculated explicitly using tensor-like relations.

For a modeling of a thin plate, a 48 d.o.f. plate element is developed with a two-dimensional beam×beam plate element. The element is the direct generalizations of 16 d.o.f. element usually used in the finite element method. The Kirchhoff plate theory with nonlinear strain-displacement relationships was used to calculate elastic forces as well as differential geometry of surfaces in 3D space to calculate mid-plane deformations and transverse curvatures and twist.

For the modeling of material damping and air resistant damping, the Rayleigh's proportional damping was employed to account for resistance forces. To choose the constants in the proportional damping, we carried out oscillations of a cantilever beam and a thin plate with an end-point weight attached. Furthermore, we obtained experimental data on the large deflections of a 2D beam and a thin plate to verify the results generated by ANCF. To the best of the authors' knowledge, this paper is the first to compare data from simulations and real experiments on large deformations of beams.

The paper is organized as follows. A description of our experimental setup for a beam is explained in chapter 2, and the results from the experiments and computer simulations of a beam are compared in chapter 3. An experimental setup for a plate is explained in chapter 4, and results from the experiments and computer simulations of a plate are compared in chapter 5, and the conclusions are listed.

† Corresponding author
CAElab, NRL, Pusan National University
E-mail : wsyoo@pusan.ac.kr
TEL : (051)510-2328 FAX : (051)512-2328

2. Experiments of Large Deflection of 2D Beam

The large deflection experiments of a beam focus on the motion of a cantilever beam with a weight attached to the free end as presented in Fig. 1.

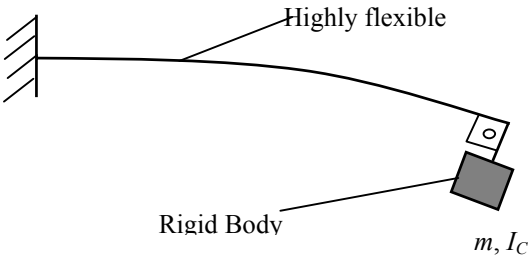

Fig. 1 Cantilever beam with attached mass

2.1 Experimental Setup with a High Speed Camera

An accelerometer is usually used to measure accelerations and displacements. However, the beam used in this research is too thin to install an accelerometer. Therefore, a high-speed camera (REDLAKE Motion Scope type), which runs up 1000frames per second, is used to measure motion.

The beam used in this test has diameter of 1mm, and are made of industrial spring steel. To make it a cantilever, the beam is clamped tightly by a heavy jig, and is held in place by two thick steel blocks. The mass of the clamp is 1.74kg, which is 1700 times heavier then the mass of the beam. Moreover, the clamp is secured with 4 bolts, which ensures a cantilever beam.

To track the end point deflection, a tracking mark was bonded at the tip. The experimental setup was installed as shown in Fig. 2, and deflections were captured by a high-speed camera.

2.2 Free Vibration to Calculate Young's Modulus and Damping Ratio

The stiffness of the beam (i.e., Young's modulus E), which is its most important material property, is calculated by an indirect method rather than a tensile test. Because the beam is too thin to fix at the tester, it is difficult to conduct such a test properly. Therefore the beam's stiffness is calculated using its measured first mode and its density. The first step is to measure the deflection of beam; the second is to calculate the first frequency of the cantilever beam. The third one calculates the stiffness using relationship between the frequency and the material's properties. The first frequency for the beam was obtained from the FFT of the free vibration, which is shown in Fig. 3. From the Fig. 3, the first frequency of the beam is obtained as 4.315Hz.

The stiffness of the beam can be calculated from the frequency of the first mode as seen in [1]

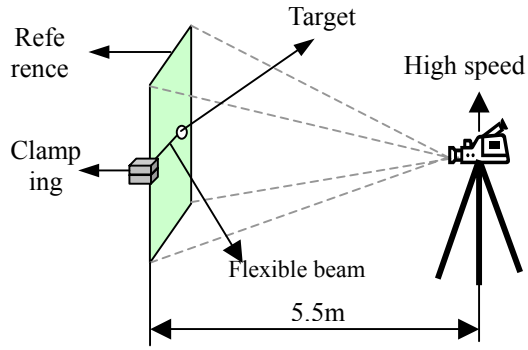

a) location of high-speed

b) lighting c) deformed

Fig. 2 Experimental setup

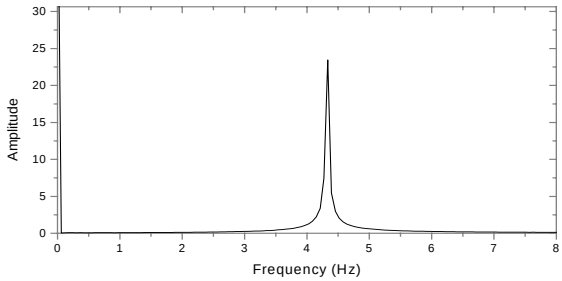

Fig. 3 The first frequency

$$\omega = (\beta l)^2 \sqrt{\frac{EI}{\rho A l^4}}, \tag{1}$$

where $\beta_n l$ represents the initial constraints of the beam. The stiffness can then be calculated according to the formula found in [2]:

$$E = \frac{\omega^2}{(\beta l)^4} \rho A l^4 \frac{1}{I}. \tag{2}$$

The calculated value E of the 1mm diameter beam was 200 GPa. Next, the damping ratio must be calculated for the simulation. To model the damping, a particular form of proportional Rayleigh damping [4] is employed and the system damping matrix assumes the following form:

$$\mathbf{D} = \alpha \mathbf{M} + \beta \mathbf{C} \tag{3}$$

which includes the mass matrix **M** and the stiffness matrix **C** multiplied by the coefficients defined below:

$$\alpha = \frac{2\omega_1\omega_2\,(\zeta_1\omega_2 - \zeta_2\omega_1)}{\omega_2^2 - \omega_1^2}, \qquad \beta = \frac{2\,(\zeta_2\omega_2 - \zeta_1\omega_1)}{\omega_2^2 - \omega_1^2} \tag{4}$$

which themselves depend on the frequencies ω_1 and ω_2, as well as on the damping ratios ζ_1 and ζ_2 for the first two modes of the system that appear from the dynamic modal equations:

$$\ddot{x}_i + 2\zeta_i\omega_i\dot{x}_i + \omega_i^2 x_i = 0\,.$$

The ratios ζ_1 and ζ_2 should be calculated from the experimental data. These coefficients depend on the damping ratios ζ_1 and ζ_2 for the first lower modes of the oscillations. The first ratio is calculated in accordance with the formula from reference [5].

$$\zeta_1 = \frac{\delta_1}{2\pi}\left(1 + \frac{\delta_1}{2\pi}\right)^{-1/2}.$$

where δ_1 is the logarithmic decrement. In case of low-level damping (such as this one), when $\delta_1 << 2\pi$, we can use the simplified expression

$$\zeta_1 \approx \frac{\delta_1}{2\pi}\,.$$

The logarithmic decrement δ_1 can be estimated from the experimental sequence of magnitudes using the simple relationship below.

$$\delta_1 = -\ln\Delta_1\,,\ \Delta_1 \approx \left(\frac{A_n}{A_1}\right)^{1/n-1}. \tag{5}$$

2.3 Large Deformation of 2D Beam

A measured mass was attached to the end of a beam to induce large deformation and a circular target point was glued on to track the beam's displacement. The mass at the end of the beam is supported until the test begins: it is released when the camera starts rolling.

The shape and location of the attached mass are shown in Fig. 4, and the parameters of the various objects used in this test are provided in Table 1.

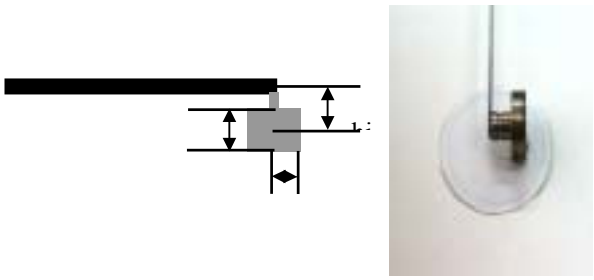

Fig. 4 Attached mass

Table 1 End-body parameters

Body №	Descrip Tion	m_0 mass g	Shift of mass center, mm		I_C mass inertia moment $kg{\cdot}m^2$
			ρ_{Cx}	ρ_{Cy}	
1	paper target	0.023	0	0	$\sim 10^{-10} \approx 0$
2	Attached mass	20.0	0	-13	$1.58{\cdot}10^{-6}$

Since the paper target's mass is very small, its effect on the results of the large deformation test is negligible. However, for the deflection without attached mass, the target's mass should be considered. A photograph of a large deformation of the beam is shown in Fig. 5. Not surprisingly it shows much deformation due to effect of the attached mass. The results of the endpoint deflections are measured 336mm, and the natural frequency of the beam was found 1.204Hz by using the FFT process.

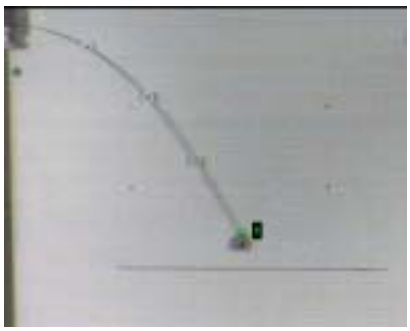

Fig. 5 A beam after a test of large deformation

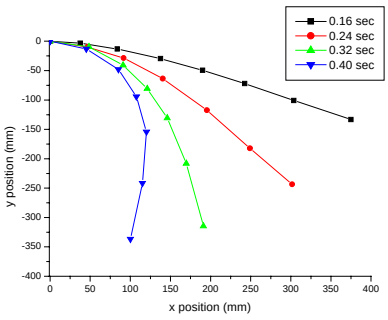

Fig. 6 Shapes and chronologies of the large deformations (1mm diameter, 20g attached mass)

The maximum displacement in the vertical direction is about 86% of the beam's length. The shapes and chronologies of these deformations are presented in Fig. 6.

After conducting the test of large deformation, the beams were retested to measure their plastic deformation. As the beams returned back to their original positions when the attached masses are removed, there was no plastic deformation.

3. Comparison of Simulation and Experiment with 2D Beam

Let us perform these calculations for the following case: the beam with diameter $d = 1\ mm$ and end-point mass $m_0 = 20\ g$ of the target. With the following values from experiments, $\omega_1 = 6.7\ rad/s$, $\omega_2 = 33\ rad/s$, $\Delta_1 = 0.987$, and $\zeta_1 = \zeta_2 = 0.002$, constants α and β are calculated as $\alpha = 0.02\ s^{-1}$, $\beta = 1 \cdot 10^{-5}\ s$, respectively. One can see that the value of β is much smaller than that of α. It is thus natural to try to ignore the stiffness-proportional part of the damping forces [4] and use the simpler damping matrix:

$$\mathbf{D} = \alpha \mathbf{M}. \qquad (6)$$

Numerical integration shows that the results obtained by both models and equation (6) differ only in 4^{th}-5^{th} significant digits. However, the integration step in the case of the full damping matrix produces a value that is 20 times smaller because the equations of motion are much stiffer in that case. This is why the simplified model of damping forces (6) is used in the numerical examples below. As can be seen in Fig. 7, the simulation result shows a nice agreement.

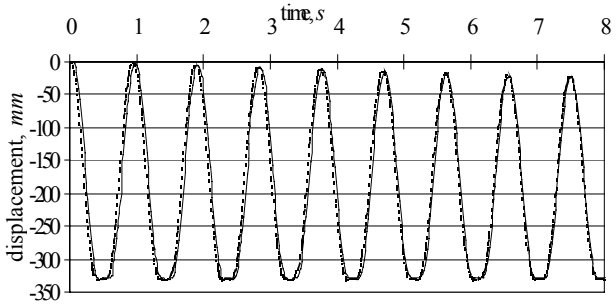

Fig. 7 Comparison of experiments and simulation

4. Experiments of a Thin Plate Oscillation

This section focuses on the large motion of a thin plate with a weight attached to the free end.

4.1 Experimental Results of a Plate

The experimental setup for the plate oscillation is shown in Fig. 8. The camera traces the target fixed at the tip. Since the motion occurs in a three dimensional space, the distance from the camera to the target is changing when the deflection occurs. Thus, the camera is installed as far as possible to reduce this kind of visual distance error. Since the camera is installed 10m from the target in the experiments, the maximum error is less then 2.5% when the deflection is about 25mm.

The tip position of a 400mm*204mm plate with 400g of attached mass is shown in Fig. 9, and the x, y, and z positions in time domain are shown in Fig. 10.

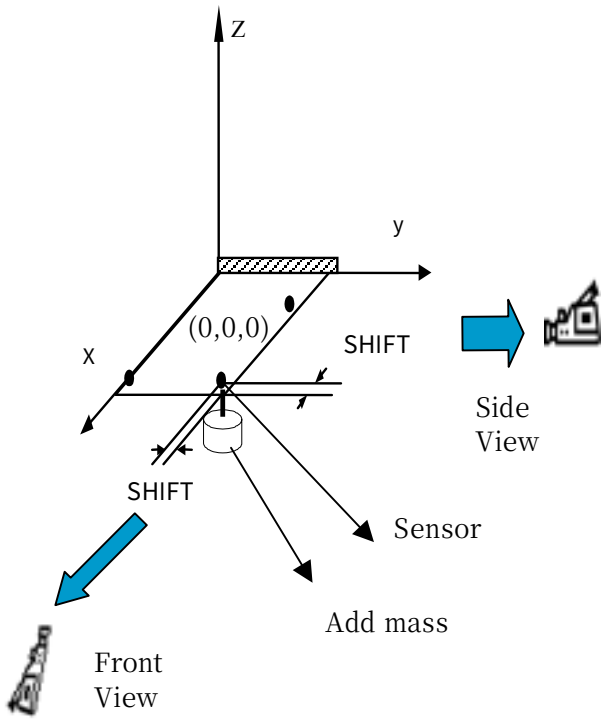

Fig. 8 Experimental setup for a thin plate

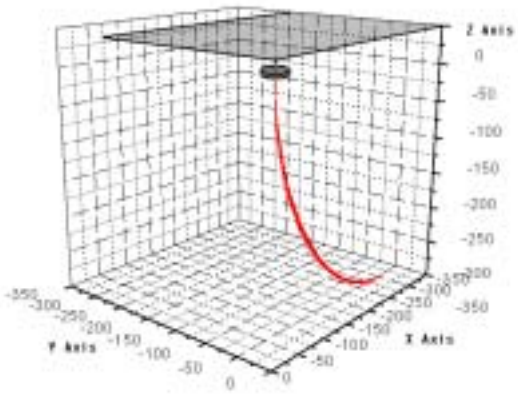

.Fig. 9 Tip position in space

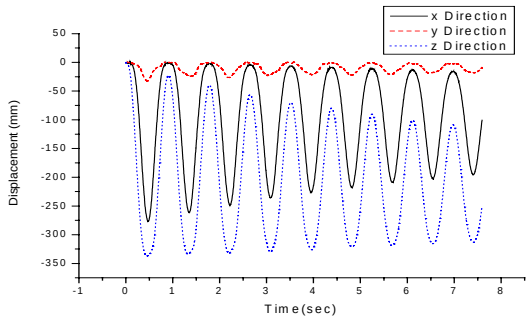

Fig. 10 Tip positions in time domain

4.2 Frequency and Damping Ratio for the Simulation

To verify the natural frequencies of the plate, the time domain data are transformed by FFT which is shown in Fig. 11. The first and the second modes are clearly shown, and the first modal frequency is about 1.2Hz. And this value of the frequency is used to calculate the Young's modulus E of the plate, which is used for the input data in the simulation.

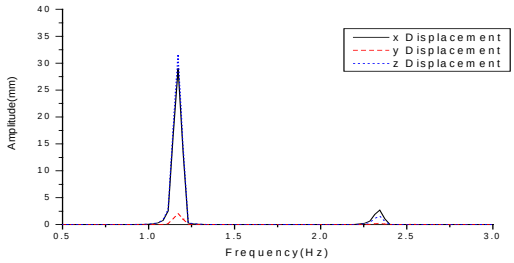

Fig. 11 Natural frequency of the plate

To determine the damping ration of the plate, the response in the time domain is captured for 32 seconds. And the damping ratio calculated using the following formula are used in the simulation.

$$\zeta = \frac{1}{\omega_n m \tau_d} \ln \frac{x_1}{x_{m+1}} = \frac{1}{\omega_n (t_{m+1} - t_1)} \ln \frac{x_1}{x_{m+1}} \qquad (7)$$

5. Comparison of Simulations and Experiments of a Thin Plate

5.1 Free Oscillation of a plate

In Fig. 12, the experimental and calculated results of the vertical displacements of the plate's end-point in free vibration are compared. The experimental curve is drawn with a solid line, while the calculated one curve is drawn with a dashed line. As one can see in Fig. 12, the two kinds of results (measured and computed) agree nicely.

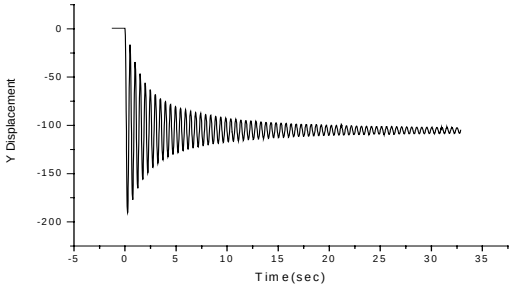

Fig. 12 Free oscillation of the plate

5.2 Oscillation with an Attached Mass

Figure 13 presents the results for the 400mm*204mm plate with 400g of attached mass. The simulation results and experimental results are compared in Fig. 16. As shown in Fig. 16, x and z positions are in a good agreement. After a few seconds, there are some time lags between two results. The reason, the authors suppose, may came from the values of Young's modulus and damping ratio but the differences are not too big.

The y position shows some deviations, but it is not a big deal if one verifies that the maximum magnitude of the y-directional deflection is very small.

Thus, the large deflection simulation of a beam with ANCF formulation and the experimental results are in a good agreement.

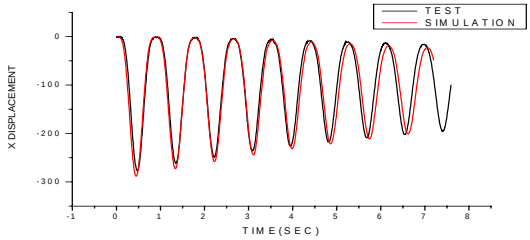

(a) x positions

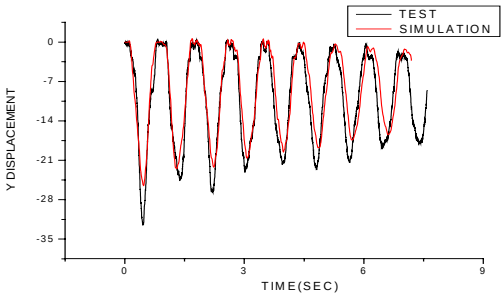

(b) y positions

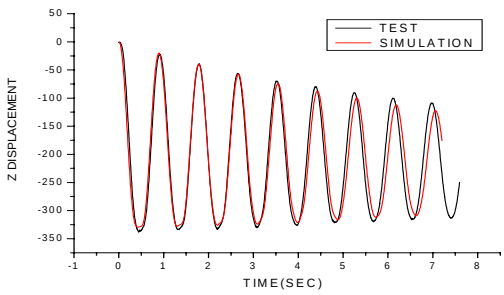

(c) z positions

Fig. 13 Comparison of experiments and simulation (plate, tip mass 400g)

6. Conclusions

In this paper, experiments and simulations of a 2D cantilever beam and a thin plate with an attached end-point weight are compared. To input a precise data for the material damping and air resistant damping in the simulation, we carried out several experiments.

Rayleigh's proportional damping was applied to account for resistance forces in large oscillation cases. It was found that when such resistance forces are small, it is possible to ignore the stiffness-proportional part of the damping forces and focus exclusively on the mass-proportional part.

To the best of the authors' knowledge, this is the first paper to compare the results of simulations and experiments in this context. Thus we have obtained some new results during this investigation.

We used the ANCF (absolute nodal coordinate formulation) for modeling of 2D beam and suggested a vector-algebra notation for the components of the vector of the nodal coordinates. To simulate the plate oscillation, we developed a new 48 dof plate element from beam*beam element. The comparison of simulation to experiment with a thin plate oscillation also showed a nice agreement.

Acknowledgements

The authors would like to thank the Ministry of Science and Technology of Korea for its financial support through a grant (M1-0203-00-0017) under the NRL (National Research Laboratory) project.

References

(1) Omar, M. A. and Shabana, A. A., 'A Two-Dimensional Shear Deformation Beam for Large Rotation and Deformation', in *Journal of Sound and bration* 243(3), 1.

(2) Mikkola, A. M. and Shabana, A. A., 'A New Plate Element based on the Absolute Nodal Coordinate Formulation', in *Proceedings of ASME 2001 DETC,* Pittsburgh, 2001.

(3) Craig, R. R., *Structural Dynamics*.

(4) Bathe, K.-J., *Finite Element Procedures*, Prentice Hall, New Jersey, 1996.

(5) Meirovitch, L, *Analytical Methods in Vibrations*, Macmillan Publishing Co., Inc., New York, 1982.

(6) Wan-Suk Yoo, Jeong-Han Lee, Jeong-Hyun Sohn, Su-Jin Park, Oleg Dmitrotchenko and Dmitri Pogorelov, 'Large Oscillations of a Thin Cantilever Beam: Physical Experiments and Simulation using Absolute Nodal Coordinate Formulation', accepted for the Nonlinear Dynamics

(7) Dmitrotchenko, O. N., 'Efficient Simulation of Rigid-Flexible Multibody Dynamics: Some Implementations and Results', in *Proceedings of NATO ASI on Virtual Nonlinear Multibody Systems* 1, W. Schielen and M. Valášek (Eds.), Prague, 2002, 51-56.

(8) Pogorelov, D., 'Some developments in computational techniques in modeling advanced mechanical systems', in *Proceedings of IUTAM Symposium on Interaction between Dynamics and Control in Advanced Mechanical Systems*, D. H. van Campen (Ed.), Kluwer Academic Publishers, Dordrecht, 1997, 313-320.

(9) Dmitrotchenko, O. N., 'Methods of simulating dynamics of hybrid multibody systems with taking into account geometrical nonlinearity', in *Dynamics, strength and reliability of transport machines*, B. G. Keglin (Ed.), Bryansk State Technical University, Bryansk, 2001, 24-34 (in Russian).

(10) Wan-Suk Yoo, Jeong-Han Lee, Jeong-Hyun Sohn, Su-Jin Park, Oleg Dmitrotchenko and Dmitri Pogorelov, 'Large Deflection Analysis of a thin plate with ANCF: Computer Simulation and Experiments', to appear in the proceeding of ECCOMAS Thematic Conference Multibody 2003, Lisbon, Portugal, July 2003